ARCHIVES
of
FOUNDRY ENGINEERING

10.24425/afe.2024.149255

Published quarterly as the organ of the Foundry Commission of the Polish Academy of Sciences

ISSN (2299-2944)
Volume 2024
Issue 1/2024

88 – 93

11/1

Copper Beam Electron Alloying with Ti Powder

P.E. Smolarczyk [a,*], M. Krupiński [a], M. Węglowski [b], W. Pakieła [a], P. Śliwiński [b]

[a] Department of Engineering Materials and Biomaterials, Silesian University of Technology, Konarskiego 18A, 44-100 Gliwice, Poland

[b] Łukasiewicz Research Network – Upper Silesian Institute of Technology, Bł. Czesława 16-18, 44-100 Gliwice, Poland

* Corresponding author: E-mail address: paulina.smolarczyk@polsl.pl

Received 06.12.2023; accepted in revised form 05.02.2024; available online 18.03.2024

Abstract

The paper presents the effect of electron beam alloying on the surface of a copper flat bar (M1Ez4) with titanium powder. Due to the quality of the surface after alloying and the obtained properties, the parameters used were given which met the assumed conditions to the greatest extent. The microstructure and mechanical properties as well as the chemical composition of surface-modified electron-beam copper show improved mechanical properties, i.e. hardness and abrasion resistance. This article uses research techniques using scanning electron microscopy and analysis of chemical composition in micro-areas (EDS). In order to examine the properties of the material after electron beam modification, hardness measurements were performed at low loads (HV0.1), abrasion resistance was tested, and conductivity was also measured. As a result of modifying the chemical and phase composition of M1E copper using an electron beam, the hardness increased by 46%, while the conductivity decreased by 16% due to the formation of intermetallic phases during solidification.

Keywords: Copper, Beam electron alloying, Abrasion resistance, Conductivity

1. Introduction

The most well-known process using an electron beam is welding or alloying, in which often the implementation of the process can be carried out without additional material. The process can be conducted with an additional material, which is fed in the form of wire or powder. In the case of welding process, in many studies there are two zones: the melting zone (weld) and the heat influence zone [1-5].

Extensive research describe the properties and structure of the obtained surfaces in laser modification processes, in which the focus was on obtaining better parameters of hardness, abrasion resistance or corrosion resistance [6-11].

Copper is a material with a very good thermal and electrical conductivity as well as excellent plasticity and corrosion resistance. However, it has poor mechanical properties, such as hardness or abrasion resistance. Some applications require improvement of mechanical properties without significant loss of electrical and thermal conductivity. Cu-Be alloys have significant mechanical properties and high level of electrical conductivity; therefore, it is applied for springs production, electrodes or electrical elements. Due to its carcinogenic properties, other alloys are often used. The second commonly used copper alloys are Cu-Ti alloys. Depending on the atomic concentration of titanium it can obtain high mechanical properties with a minimal decrease of electrical conductivity or increase mechanical properties at the expense of conductivity [12].

One of the possibilities to improve the modification of metal surfaces is laser modification, in this case there is a wide range of possible types of lasers, e.g. HPDL diode, fiber, CO_2 or Nd:YAG lasers [13-14].

Electron Beam Processing technologies are both precise and efficient. In comparison to conventional methods, electron beam techniques boast a notably brief technological processing time. Moreover, there is a uniform distribution of electron beam energy, and the meticulous control of beam parameters results in the precise formation of materials with specific structures and properties. Another advantage of electron beam modification is a large variety of possible material combinations and an elimination of finishing treatment (mechanical and thermal processing). In the case of electron beam welding, it is possible to obtain a greater depth of melting, a high welding speed as well as cleaner welds compared to other conventional welding methods. These methods are part of additive techniques, which makes it possible to produce materials with exceptional performance characteristics [15, 16]

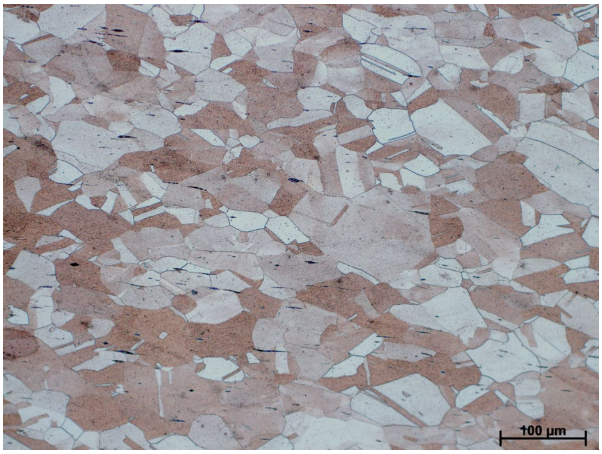

Fig. 1. Microstructure of copper flat bar, cross-section view, brightfield observation, magnification 200x.

As a result of modifications of copper surfaces using laser technologies, three characteristic zones are created: the melting zone, the heat impact zone and the recrystallization zone [17].

The Phase equilibrium system Cu-Ti (Fig. 1) indicates the possibility of different intermetallic phases – Cu_4Ti, Cu_2Ti, Cu_3Ti_2, Cu_4Ti_3, CuTi, $CuTi_2$ and $CuTi_3$.

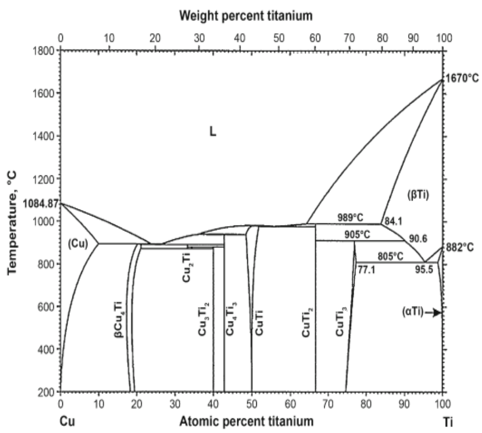

Fig. 2. Cu-Ti phase equilibrium system [18]

The resulting phases have a profound impact on the performance properties. Studies [19] show that the occurrence of the Cu_3Ti phase may reduce the strength of the modified material, in addition, the electrical conductivity of Cu-Ti alloys in this case decrease and due to the high concentration of Ti in the Cu matrix. Laser modification of the copper surface using titanium [17], in which the Cu_3Ti_2 phase was found, shows an almost fourfold increase in hardness and a reduction in consumption by more than 53%.

Bearing in mind the application possibilities of the electron beam presented above, the work focused on the impact of alloying technology on the mechanical properties of modified copper, without a significant loss in the conductivity of a material.

2. Materials and experiments procedure

In order to investigate the effect of electron beam alloying on the copper surface, the following steps were performed:

The copper flat bar (M1Ez4) with a rectangular cross-section (30x10 mm) and a 99.95% purity was supplied by Kafra Color Metals Company (Poland). Microstructure of copper flat bar was shown on Fig. 1 in cross-section Chosen flat bar was sanded with sandpaper with a 500 grit. Then, a mixture of Cu and Ti powders mixed in isopropyl alcohol was applied to the surface of the flat bar. In the next step, the prepared material was left to evaporate the alcohol and placed on the working table of the device. The following process parameters were selected: focused length of 500 mm, a voltage of 120 kV, a cathode current of 22 A, a focal point of 649 mA, a cyclic frequency of 100 Hz, a feed speed of 500 mm / min and a beam current of 16 mA.

Structural research after the preparation of metallographic dies (grinding, polishing, etching in D2 electrolyte), was carried out using optical microscopy – Axio Observer (Zeiss) – in a bright field. The width and the depth of the melting zone were also measured using tools in the microscope's computer software.

The further part of the structural research was performed by the Zeiss Supra 35 scanning electron microscope using the secondary electron method, and the chemical composition analysis using the EDS method was also performed.

The surface roughness after the alloying process was made with the Tylor-Hubson Sutronic 25 profilometer. Roughness test parameters: measuring section length 4 mm, scale 300 µm.

A static Vickers hardness test ($HV_{0.1}$) was performed at low load, using the Future Tech FM-ARS 900 device (time 10 sec.)

An abrasion resistance test was performed using the ball-on-plate method (in reciprocating motion), at room temperature, on the CSM Instrument Tribometer device. A ceramic ball (Al_2O_3) with a diameter of 6 mm was used as an anti-sample. The process parameters are presented in Table 1.

Table 1.
Ball-on-plate test parameters

Full Amplitude [mm]	Linear speed [cm/s]	Counter-sample load [N]	Sliding distance [m]	Frequency [Hz]	Temperature process [°C]
6	2	25	25	0.53	25

The width of the abrasion profile was measured using the Zeiss Supra 35 scanning electron microscope.

In addition, the conductivity of the material before and after modification was measured using the Sigmascope SMP350 with FS40 probe. Parameters: 60 kHz probe frequency, at room temperature.

3. Results

As a result of electron beam alloying of the copper surface, "stitches" were obtained (Fig. 3).

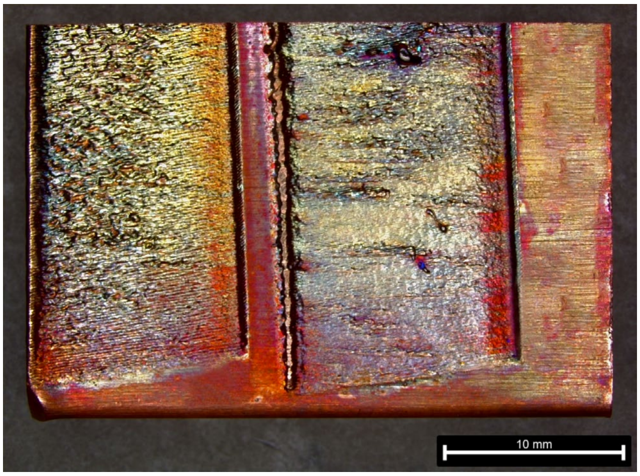

Fig. 3. Copper flat after the alloying process

The applied process parameters, as well as the properties of the powder mixture used, influenced on the appearance of the melting zone. The depth of the melting zone is contained in the range from 149 up to 206 µm. No discontinuities were detected in the top layer. Structure in the Figure 3 exhibits the characteristics of the zone melting. In addition, the specific structure of the top layer in cross-section view (Figure 4) in the surface zone was formed as a result of the rapid movement of the electron beam on the surface of the molted material.

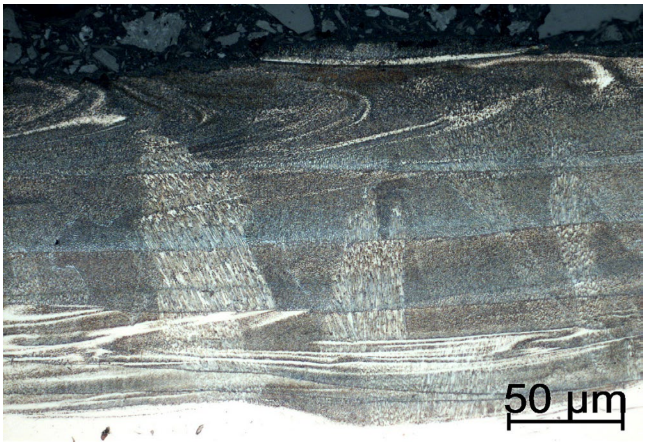

Fig. 4. Melting zone, cross-section view, brightfield observation, magnification 500x

Column structure (under the surface zone) most likely results from rapid heat dissipation towards the sample core, resulting from the supply of high power in the form of heat to the sample, by electron beam melting.

The power of the beam during melting causes low surface roughness, Fig. 5 shows average surface roughness after electron beam alloying. For the electron beam-alloyed surface, the average parameter of the arithmetic mean of the deviation from the mean line (Ra) is 0.214 µm. In addition, the average parameter of the highest height with roughness according to the measured 10 highest profiles (Rz) is 0.851 µm.

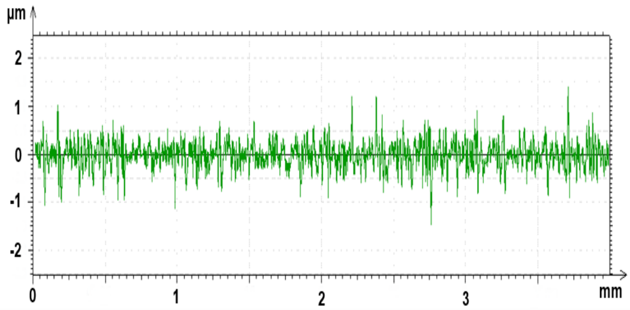

Fig. 5. Average surface roughness after electron beam alignment

Due to the surface roughness after alloying, the profilometer is not able to read the abrasion path after ball-on-plate examination, for comparative purposes, images of the abrasion path were taken using scanning electron microscopy. Figure 6a shows the copper abrasion path without modification, where the average width of the path is about 760 µm. Figure 6b shows the copper abrasion path after modification, the average width of the path after modification is about 386.5 µm.

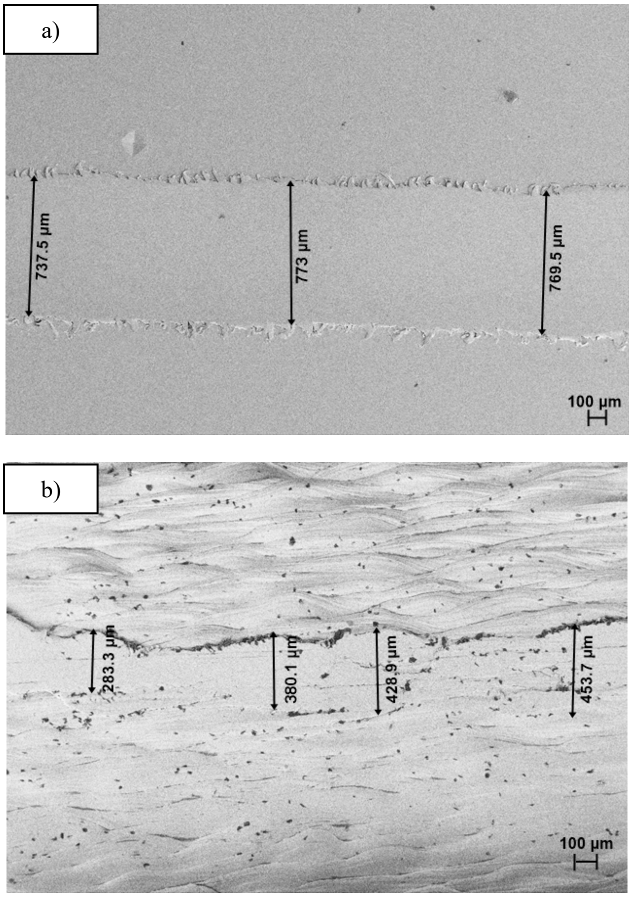

Fig. 6. Copper abrasion path: a) without modification, b) after Ti modification

Using scanning electron microscopy (SEM), EDS X-ray microanalysis was performed in areas of the top layer. SEM parameters are as follow: accelerating voltage 20kV, magnification 1000x. Figure 7 shows places for analysis in the upper part of the melting zone.

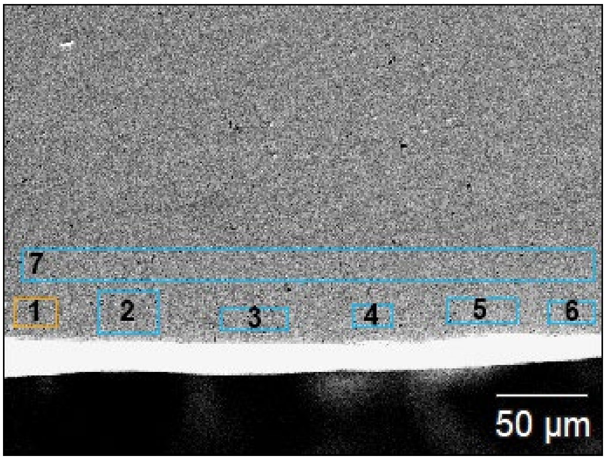

Fig. 7. EDS microanalysis, 1-7 analysis areas in the upper part of melted zone

Areas marked with numbers from 1 to 7, are located at a distance of about 10 to 85 µm from the surface of the test sample. Their chemical composition is presented in Table 2.

Table 2.
Analysis results in microareas (points marked in Figure 7)

	Atom [%]	
	Ti	Cu
#1	2.7	97.3
#2	2.3	97.7
#3	2.4	97.6
#4	2.5	97.5
#5	3.0	97.0
#6	2.7	97.3
#7	3.5	96.5

Microscopic observations and the results of EDS X-ray microanalysis revealed an even distribution of titanium introduced in the form of a paste. The proportion of titanium introduced is between 2.3 and 3.5 % atomically. The depth of titanium melting is in the range from 2 to 85 µm, no gaps in the layer were found.

Hardness tests for copper performed on surface before modification and after alloying were subjected to mathematical analysis, the mean and standard deviation were calculated, which are summarised in Table 3.

Table 3.
Statistical values of hardness test

	Cu (M1Ez4)	After alloying
Average [$HV_{0.1}$]	107.76	158.01
Mean deviation	4.20	17.92

Figure 8 shows a statistical graph in the form of a histogram, Figure 8a shows a histogram of copper without modification, Figure 8b histogram after electron beam alloying. An average increase in hardness of 50 units [$HV_{0.1}$] was noted.

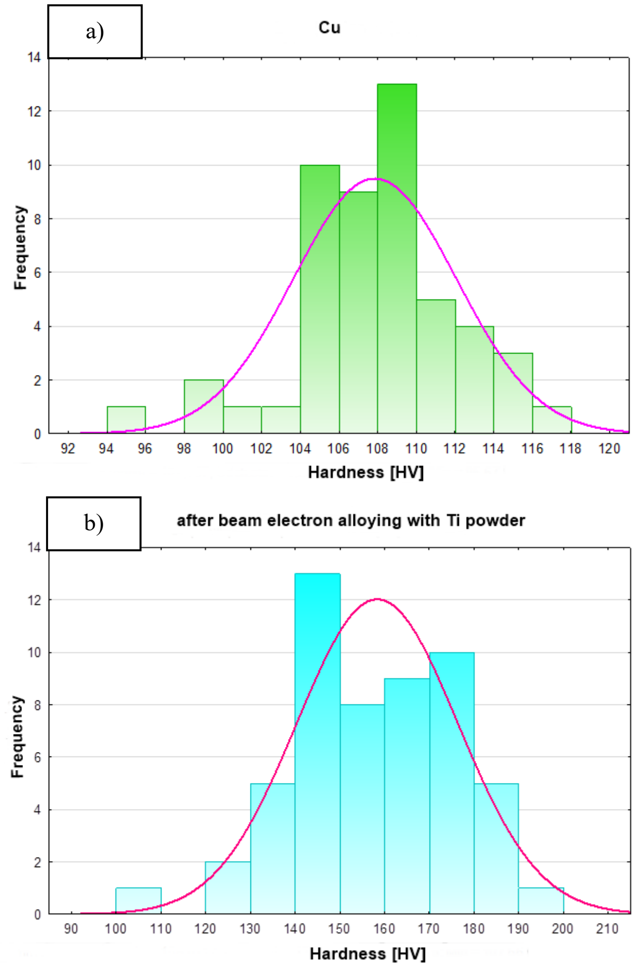

Fig. 8. Hardness histogram: a) before modification, b) after Ti alloying.

Conductivity test for copper before and after modification were subjected to mathematical analysis, the mean and standard deviation were calculated, which are summarised in Table 4.

Table 4.
Statistical values of conductivity test

	Cu (M1Ez4)	Copper after beam electron alloying with Ti powder
Average [MS/m]	59.05	49.57
Mean deviation	0.218	4.038

As a result of beam electron alloying with Ti powder average decrease in conductivity of over 10 units was noted.

4. Conclusions

Parameters of electron beam alloying of copper with titanium powder, which showed the best results in both properties and surface quality after modification.: focused length of 500 mm, a voltage of 120 kV, a cathode current of 22 A, a focal point of 649 mA, a cyclic frequency of 100 Hz, a feed speed of 500 mm / min and a beam current of 16 mA caused melting zone which is contained in the range from 149 up to 206 µm. Average depth of melting zone is about 100 µm. Compared to [17], only the presence of a melting zone and a heat-affected zone were noted, no recrystallization zone was noted, which is characteristic of the electron beam process.

As a result of surface modification on the top of copper flat obtained the average roughness of surface (R_a) at the level 0.214 µm. Comparison of the width of the abrasion path both before and after the alloying process indicates a lower intensity of wear of the alloyed material, after alloying the abrasion path is twice as narrow. The average electrical conductivity of the material after modification decreased by 16%

SEM studies showed an even distribution of Ti in the top layer, without gaps. The proportion of titanium introduced is between 2.3 and 3.5 % atomically, which causes increase the hardness by 46%, due to solidification of phases with Ti after alloying with an electron beam.

References

[1] Węglowski, M.St., Błacha, S. & Phillips, A. (2016). Electron beam welding – Techniques and trends – Review. *Vacuum.* 130, 72-92. DOI: 10.1016/j.vacuum.2016.05.004.

[2] Yunlian, Q., Ju, D., Quan, H. & Liying, Z. (2000). Electron beam welding, laser beam welding and gas tungsten arc welding of titanium sheet. *Materials Science and Engineering: A.* 280(1), 177-181. DOI: 10.1016/S0921-5093(99)00662-0.

[3] Guo, S., Zhou, Q., Kong, J., Peng, Y., Xiang, Y., Luo, T., Wang, K. & Zhu, J. (2016). Effect of beam offset on the characteristics of copper/304stainless steel electron beam welding. *Vacuum.* 128, 205-212. DOI: 10.1016/j.vacuum.2016.03.034.

[4] Zhan, X., Yu, H., Feng, X., Pan, P. & Liu, Z. (2019). A comparative study on laser beam and electron beam welding of 5A06 aluminum alloy. *Materials Research Express.* 6(5), 056563. DOI: 10.1088/2053-1591/ab0562.

[5] Zhu, Q. *et al.*, (2020). Research status and progress of welding technologies for molybdenum and molybdenum alloys. *Metals.* 10(2), 279, 1-16. DOI: 10.3390/met10020279.

[6] Pakieła, W. & Brytan, Z. (2020). Laser surface alloying of aluminum alloys with Cu/Fe metallic powders. *Solid State Phenomena*. 308, 64-75, DOI: 10.4028/www.scientific.net/SSP.308.64.

[7] Pakieła, W., Tański, T., Brytan, Z., Chladek, G. & Pakieła, K. (2020). The impact of laser surface treatment on the microstructure, wear resistance and hardness of the AlMg5 aluminum alloy. *Applied Physics A.* 126, 1-10. DOI: 10.1007/s00339-020-3350-x.

[8] Smolarczyk, P., Krupiński, M. & Pakieła, W. (2021). Microstructure and properties of the aluminum alloyed with ZrO powder using fiber laser. *Solid State Phenomena*. vol.

326, 157-165. DOI: 10.4028/www.scientific.net/SSP.326.157.

[9] Janicki, D., Górka, J., Kwaśny, W., Pakieła, W. & Matus, K. (2020). Influence of solidification conditions on the microstructure of laser-surface-melted ductile cast iron. *Materials.* 13(5), 1174, 1-13. DOI: 10.3390/ma13051174.

[10] Krupiński, M., Krupińska, B. & Chulist, R. (2023). Influence of Re on the plastic hardening mechanism of alloyed copper. *Materials.* 16(16), 5519, 1-13. DOI: 10.3390/ma16165519.

[11] Krupińska, B., Rdzawski, Z., Krupiński, M. & Pakieła, W. (2020). Precipitation Strengthening of Cu–Ni–Si Alloy. *Materials.* 13(5), 1182, 1-12. DOI: 10.3390/ma13051182.

[12] Caron, R.N. (2001). Copper Alloys: Properties and Applications. In Buschow, K.H.J., Cahn, R.W., Flemings, M.C., Ilschner, B., Kramer, E.J., Mahajan, S. & Veyssière, P. (Eds.), *Encyclopedia of Materials: Science and Technology* (pp. 1665-1668). Oxford: Elsevier.

[13] Patidar, D. & Rana, R.S. (2018). The effect of CO2 laser cutting parameter on Mechanical & Microstructural characteristics of high strength steel-a review. *Materials Today: Proceedings.* 5(9), Part 3, 17753-17762. DOI: 10.1016/j.matpr.2018.06.099.

[14] Kusinski, J., Kac, S., Kopia, A., Radziszewska, A., Rozmus-Górnikowska, M., Major, B., Major, L., Marczak, J. & Lisiecki, A. (2012). Laser modification of the materials surface layer – a review paper. *Bulletin of the Polish Academy of Sciences: Technical Sciences*. 60(4), 711-728. DOI: 10.2478/v10175-012-0083-9.

[15] Valkov, S., Ormanova, M. & Petrov, P.(2020). Electron-beam surface treatment of metals and alloys: techniques and trends. *Metals*. 10(9), 1219, 1-20. DOI: 10.3390/met10091219.

[16] Körner, C. (2016). Additive manufacturing of metallic components by selective electron beam melting — a review. *International Materials Reviews.* 61(5), 361-377. DOI: 10.1080/09506608.2016.1176289.

[17] Krupiński, M., Smolarczyk, P.E. & Bonek, M. (2020). Microstructure and properties of the copper alloyed with Ag and Ti powders using fiber laser. *Materials.* 13(11), 2430, 1-13. DOI: 10.3390/ma13112430.

[18] Božić, D., Stasic, J., Dimcic, B., Vilotijevic, M. & Rajkovic, V. (2011). Multiple strengthening mechanisms in nanoparticle-reinforced copper matrix composites. *Bulletin of Materials Science.* 34, 217-226. DOI: 10.1007/s12034-011-0102-8.

[19] Ran, Q., Liu, J., Wang, X. & Liu, J. (2021). The Effect of Heat Treatment on the Microstructure Evolution and Properties of an Age-Hardened Cu-3Ti-2Mg Alloy. *Archives of Metallurgy and Materials*. 66(1), 163-170. DOI: 10.24425/amm.2021.134772. https://journals.pan.pl/dlibra/publication/134772/edition/117801